Supplement of Weather Clim. Dynam., 4, 701–723, 2023
https://doi.org/10.5194/wcd-4-701-2023-supplement


*Supplement of*

# Validation of boreal summer tropical–extratropical causal links in seasonal forecasts

**Giorgia Di Capua et al.**

*Correspondence to:* Giorgia Di Capua (dicapua@pik-potsdam.de)

## Section S1

To check whether the results shown in Figs. 5 and 6 depend on the chosen *p*-value threshold, we have run Experiment A for each p-value in the set $P = \{0.1, 0.2, 0.3, 0.4, 0.5, 0.6, 0.7, 0.8, 0.9, 1.0\}$ for both MCA 1 and 2 and we have produced Figs. 5 and 6 for all the results. We have done so for both SEAS5 forecast data initialized on the 1st of May and on the 1st of March. The number of figures resulting from this sensitivity exercise is 80, thus we have produced a figure which summarizes the results for SEAS5 initialized on the 1st of May. Figure S9 shows the summary results for the ten histograms obtained with the selection of *p*-values in *P* for each of the original histograms shown in Fig. 5b,d,f,h and 6b,d,f,h in the main manuscript. Please see the figure caption for a detailed description of each panel. It can be seen that changing the *p*-value does not change considerably (i.e. by at most a few percent) the percentage of grid points for which $\beta_{ERA5}$ is found in each quantile category (Fig. S9). However, this figure is obtained considering only the causal patterns shown in Figs. 3, 5 and 6, which present robust causal teleconnections also shown in using ERA-Interim data in Di Capua et al. (2020) https://wcd.copernicus.org/articles/1/519/2020/

## Figures

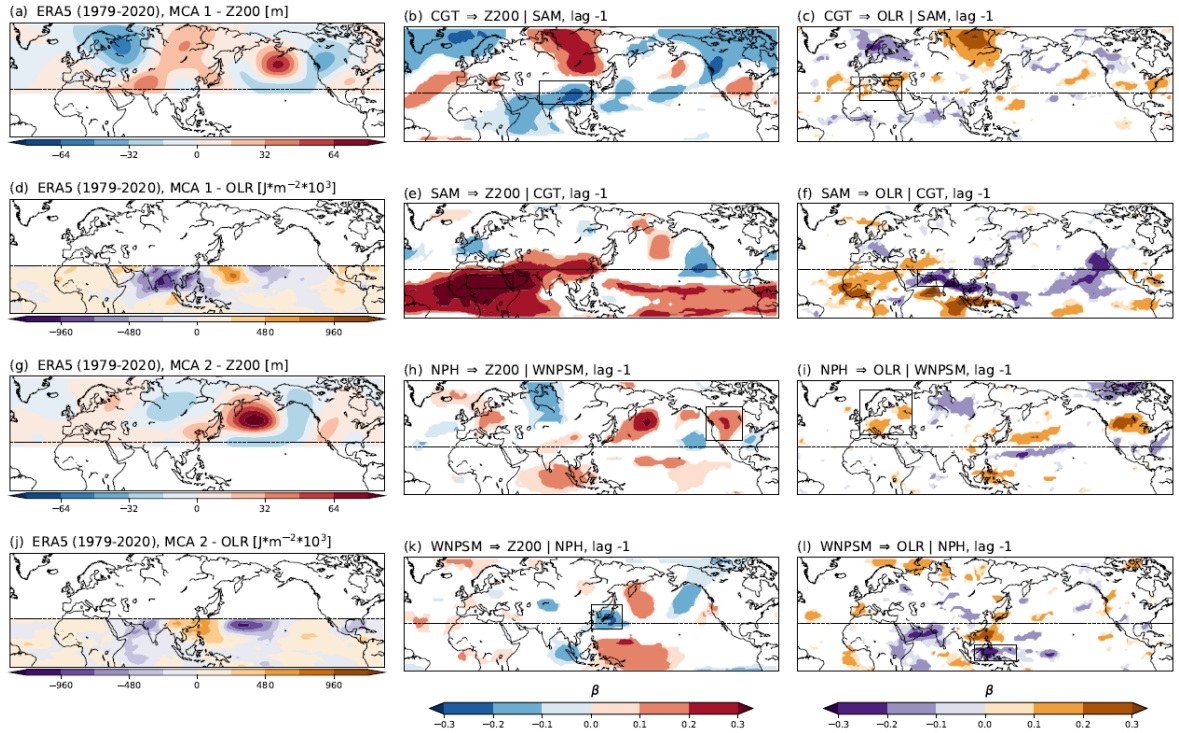


**Figure S1.** MCA modes and causal maps for ERA-L. Same as for Fig. 3 in the main text but for ERA5 data from 1979-2020.

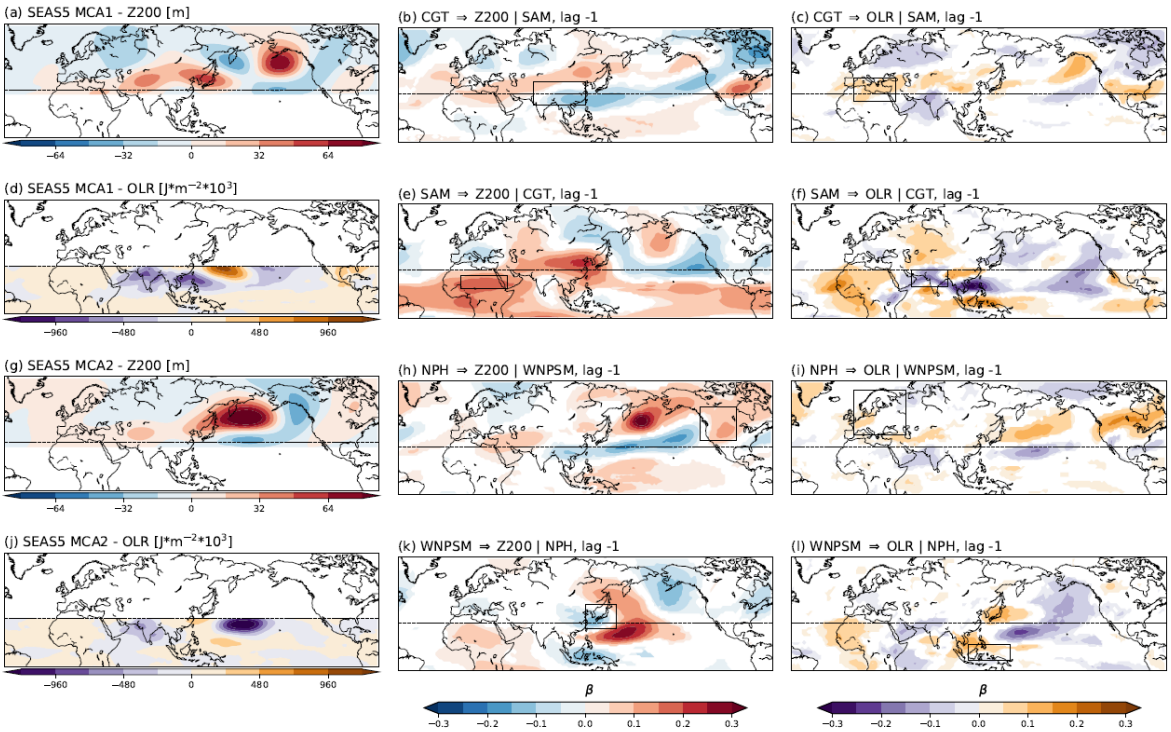


**Figure S2.** MCA modes and causal maps for SEAS5. Same as for Fig. 4 in the main text but for MCA modes obtained by running directly the MCA analysis on the SEAS5 dataset.

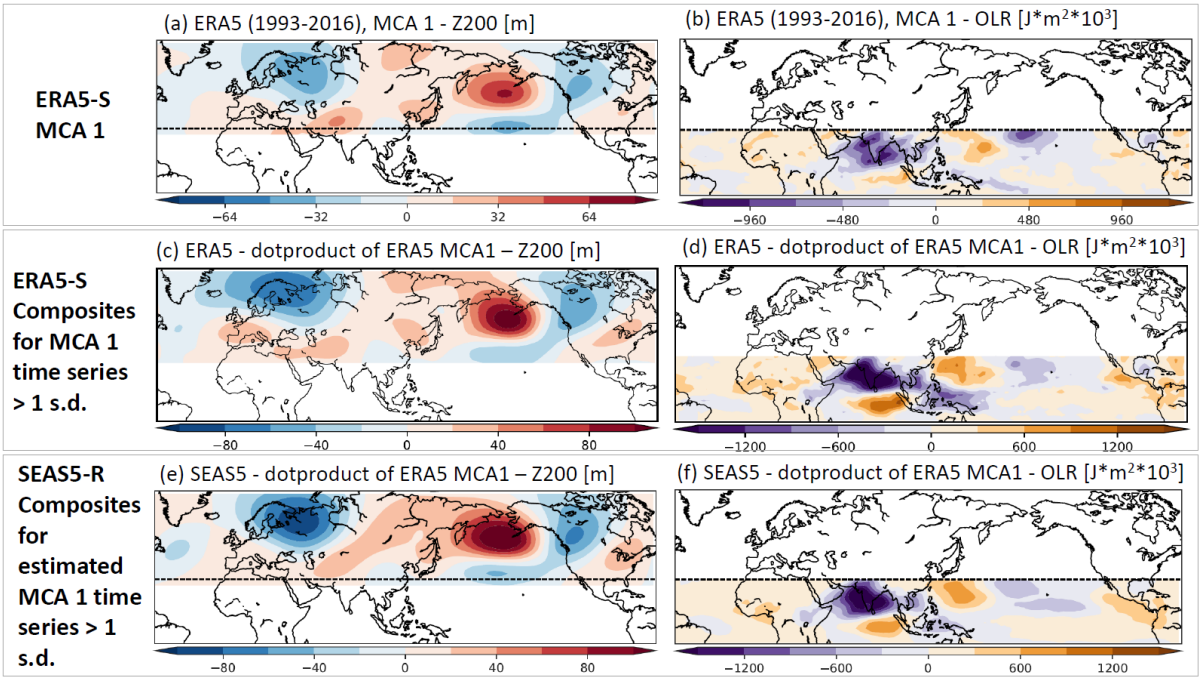


**Figure S3.** Panel (a) ERA-S MCA mode 1 Z200. Panel (b) ERA-S MCA mode 1 OLR. Panel (c) ERA-S MCA mode 1 Z200 calculated as the composites of ERA5 Z200 for MCA1 time steps with values > 1 .s.d. Panel (d) same as panel (c) but for
70 OLR field. Panel (e) SEAS5-R MCA mode 1 Z200 calculated as the composites of SEAS5 Z200 for MCA1 time steps with values > 1 .s.d. Panel (f) same as panel (c) but for OLR field.

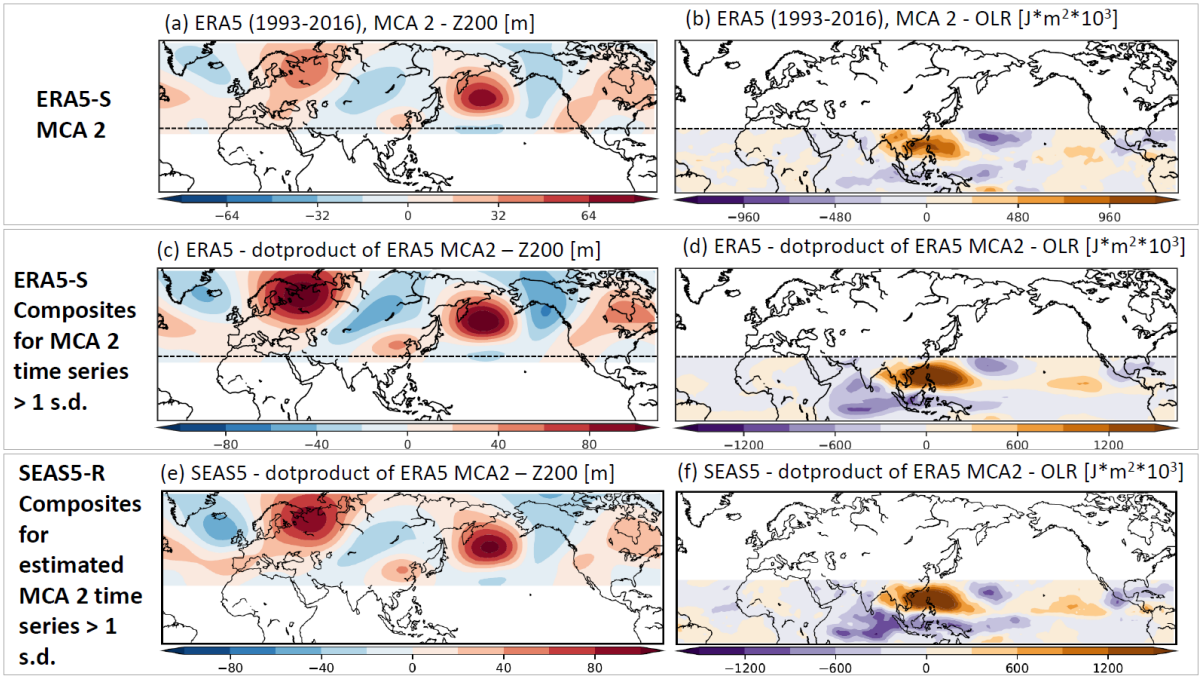


**Figure S4.** Panel (a) ERA-S MCA mode 2 Z200. Panel (b) ERA-S MCA mode 2 OLR. Panel (c) ERA-S MCA mode 2 Z200 calculated as the composites of ERA5 Z200 for MCA2 time steps with values > 1 .s.d. Panel (d) same as panel (c) but for OLR field. Panel (e) SEAS5-R MCA mode 2 Z200 calculated as the composites of SEAS5 Z200 for MCA2 time steps with values > 1 .s.d. Panel (f) same as panel (c) but for OLR field.

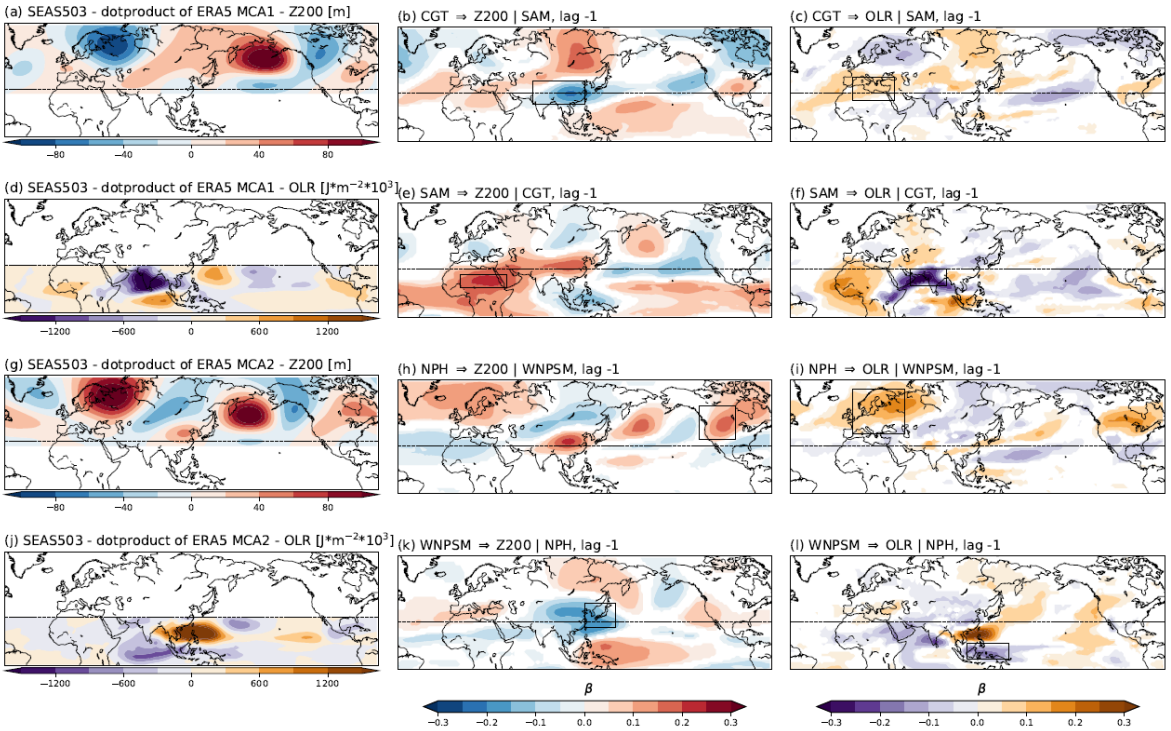


**Figure S5.** MCA modes and causal maps for SEAS5-R. Same as for Fig. 4 in the main text but for MCA modes obtained with SEAS5 dataset initialized on the 1st of March.

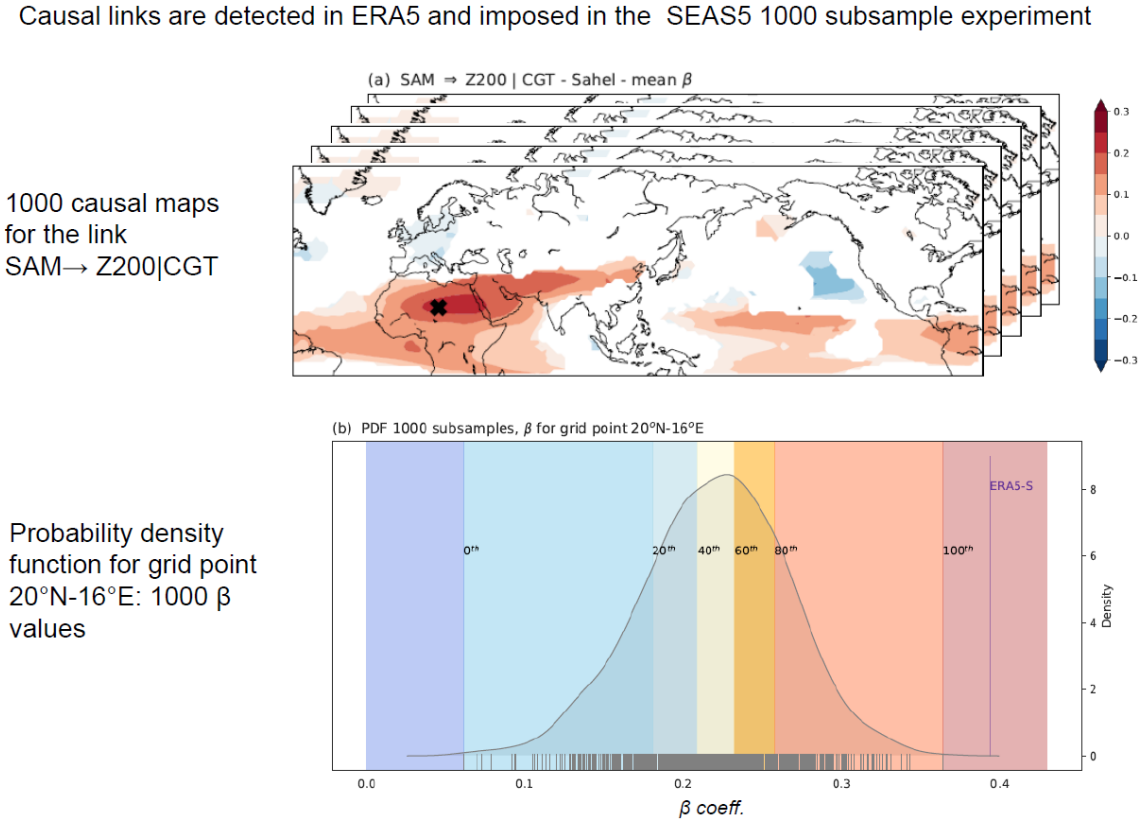


**Figure S6.** Schematic of subsampling Experiment A. Panel (a) shows an example of causal maps obtained from the 1000 subsamples. Panel (b) shows the probability density function for the 1000 $\beta$ values obtained from subsampling Experiment A for the link SAM→Z200|CGT for grid point 20°N, 16°E.

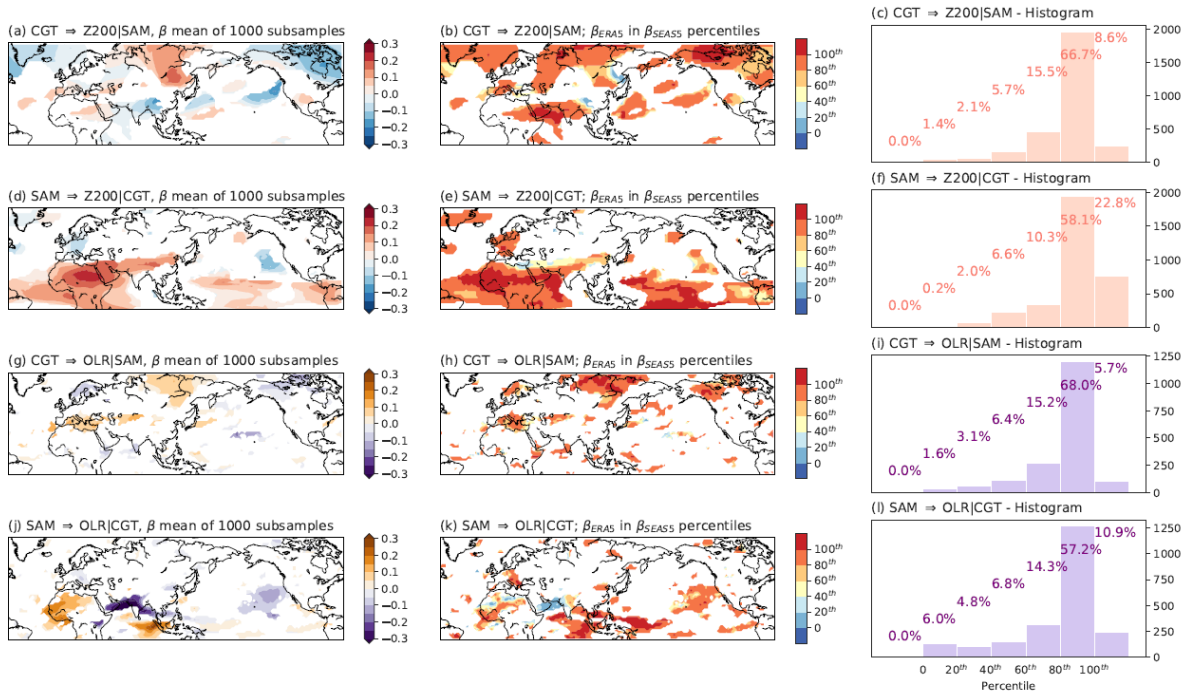


**Figure S7.** Same as for Fig. 5 in the main text but obtained with the SEAS5 dataset initialized on the 1st of March.

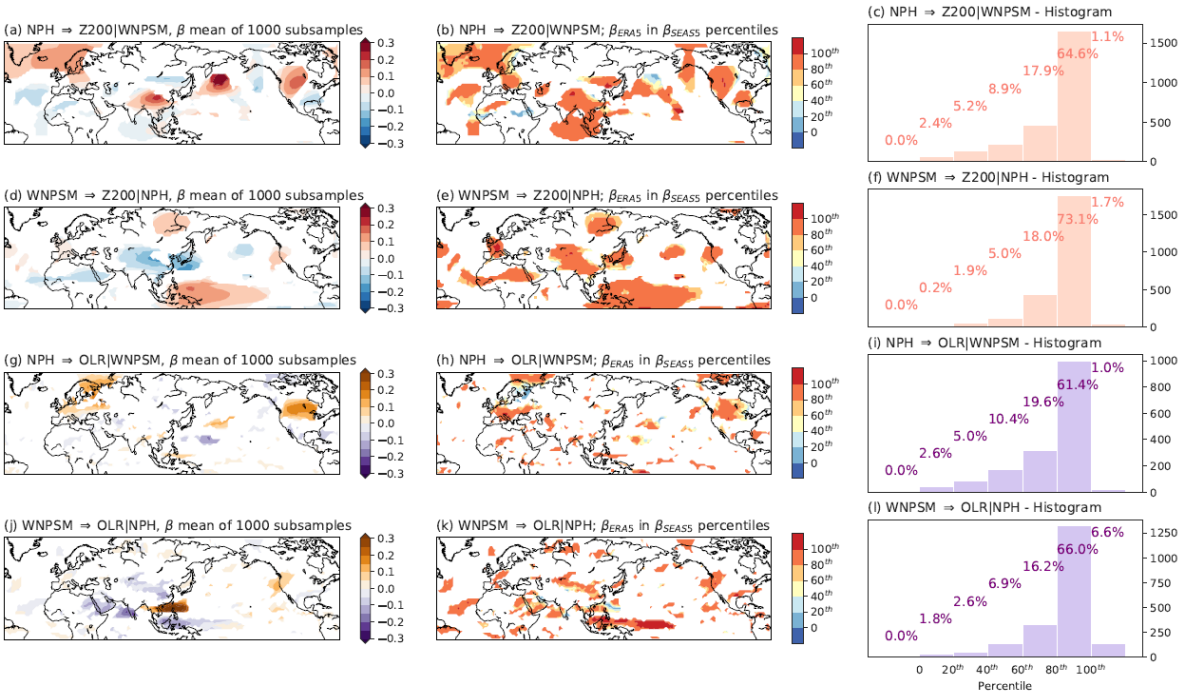


**Figure S8.** Same as for Fig. 6 in the main text but obtained with the SEAS5 dataset initialized on the 1st of March.

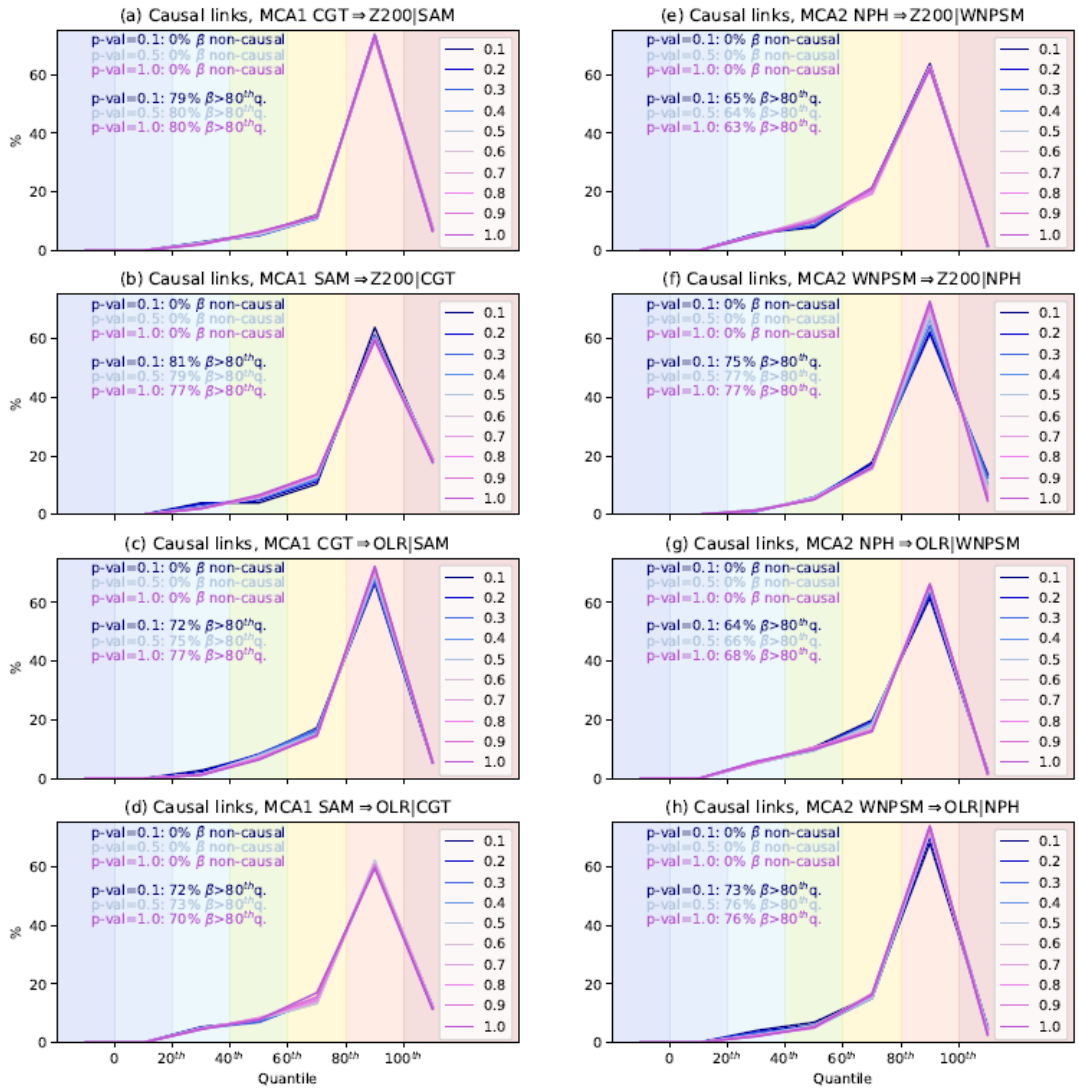


**Figure S9.** Experiment A, sensitivity test. Panel (a): Histogram showing the percentage of grid points for which $\beta_{ERA5}$ falls in a certain quantile range as obtained for $\beta_{SEAS5}$ coefficients for the link CGT→Z200|SAM. Panel (b): same as for Panel (a) but for the link SAM→Z200|CGT. Panel (c): same as for Panel (a) but for the link CGT→OLR|SAM. Panel (d): same as for Panel (a) but for the link SAM→OLR|CGT. Panel (e): same as for Panel (a) but for the link NPH→Z200|WNPSM. Panel (f): same as for Panel (a) but for the link WNPSM→Z200|NPH. Panel (g): same as for Panel (a) but for the link NPH→OLR|WNPSM. Panel (h): same as for Panel (a) but for the link WNPSM→OLR|NPH. This figure is obtained taking into account only the grid points that show significant causal links in Fig. 4 in the main text. In each panel, the percentage of non-causal grid points analysed and the percentage of grid points for which the beta values exceeds the 89th percentile is highlighted for p-values in the set {0.1, 0.5, 1.0}.

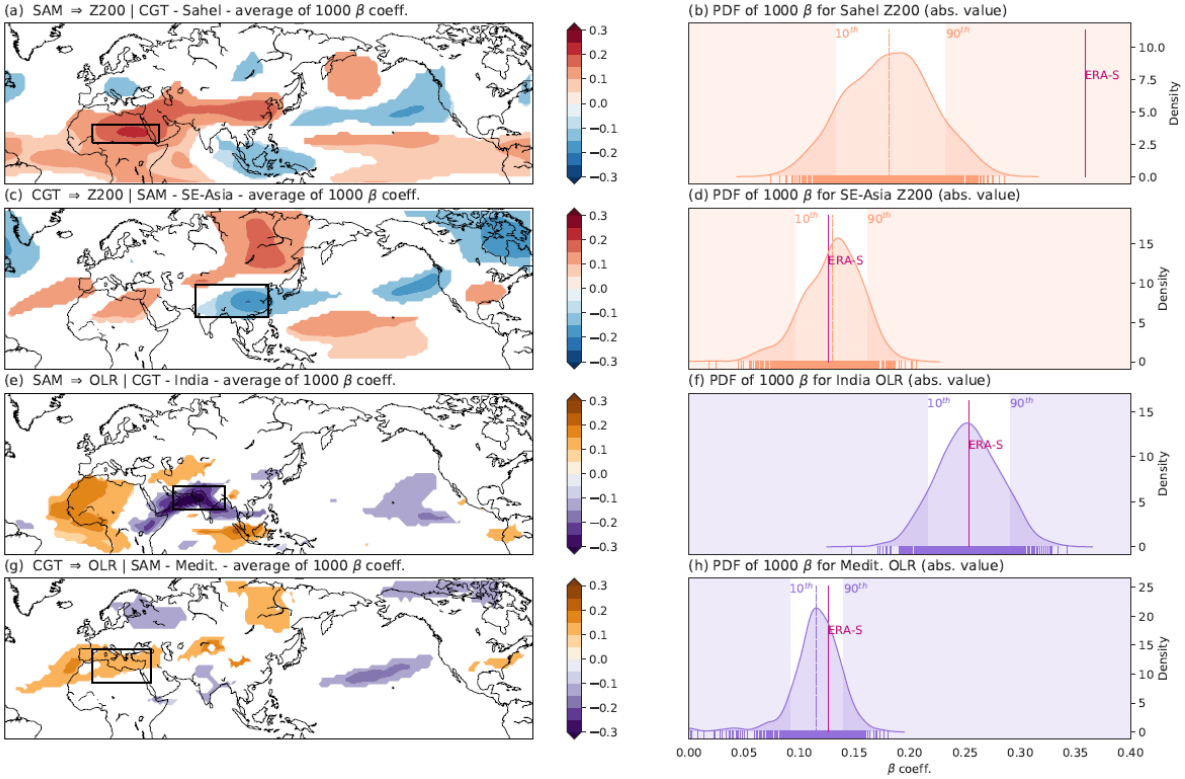


**Figure S10.** Same as for Fig. 8 in the main text but obtained with the SEAS5 dataset initialized on the 1st of March.

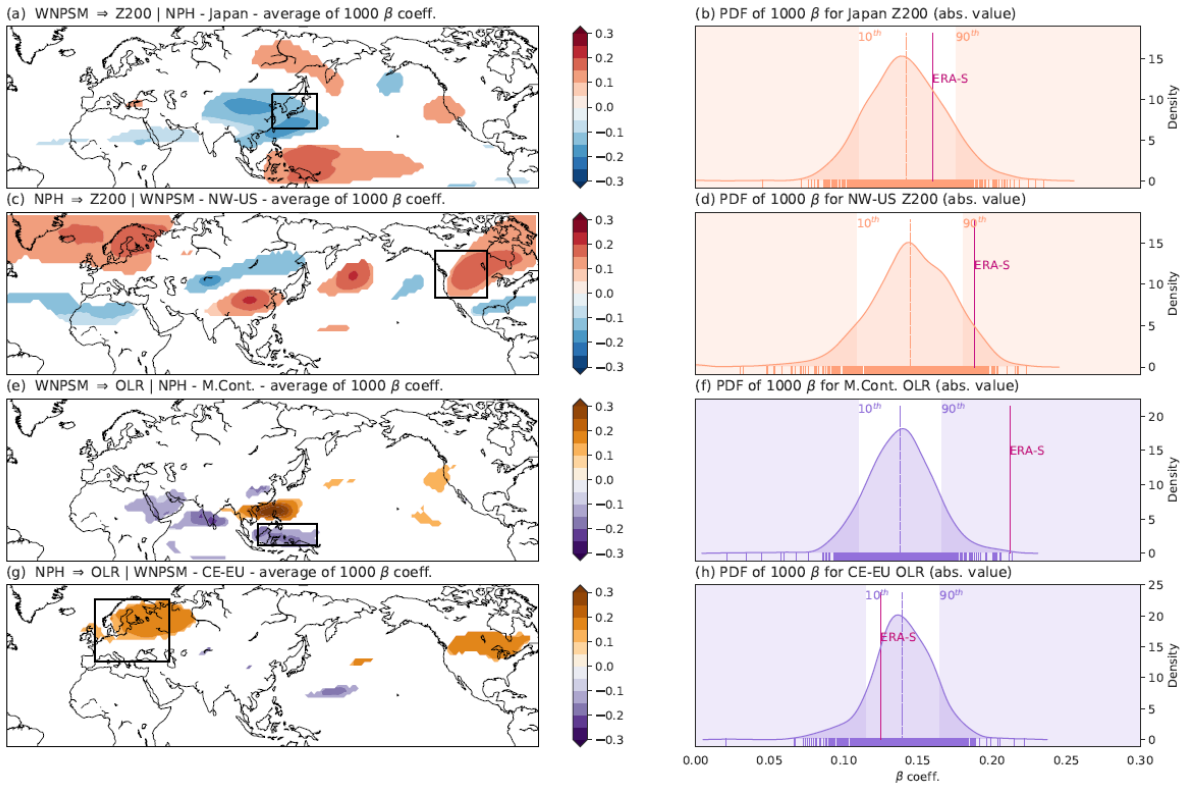


**Figure S11.** Same as for Fig. 9 in the main text but obtained with the SEAS5 dataset initialized on the 1st of March.

115

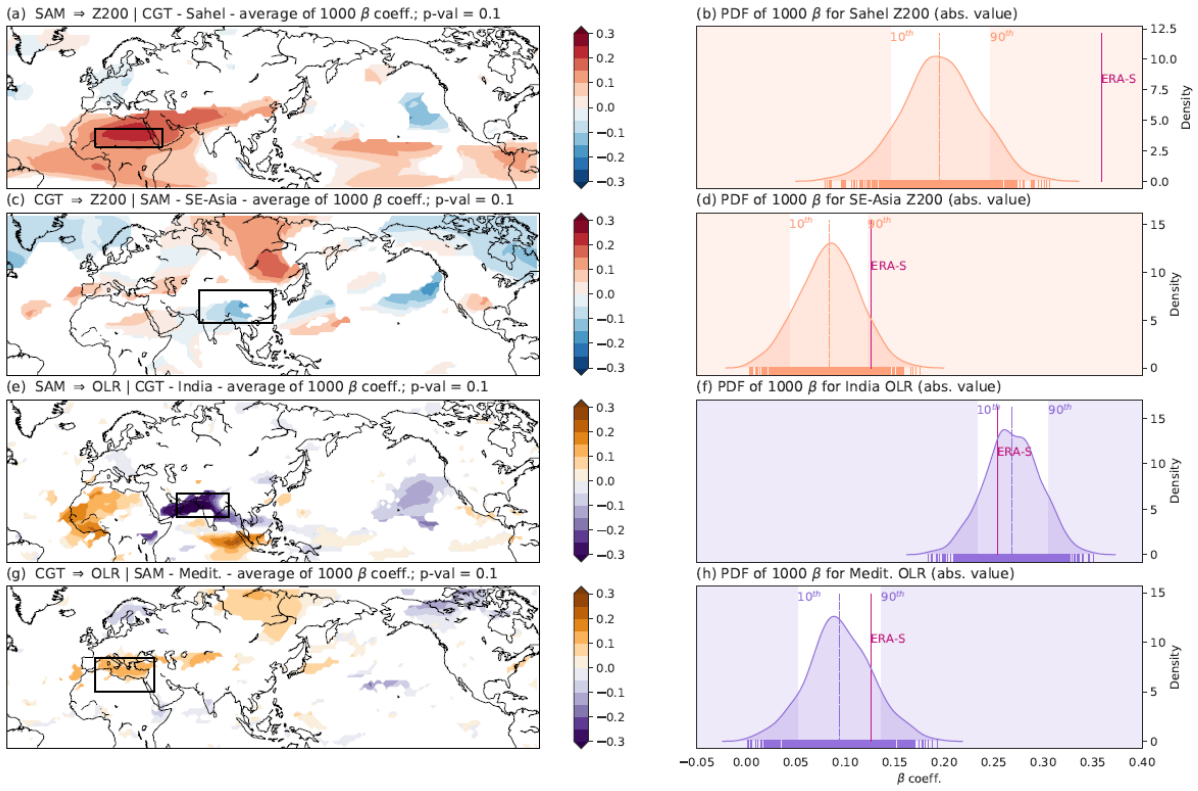


**Figure S12.** Same as for Fig. 8 in the main text but obtained with Experiment A.

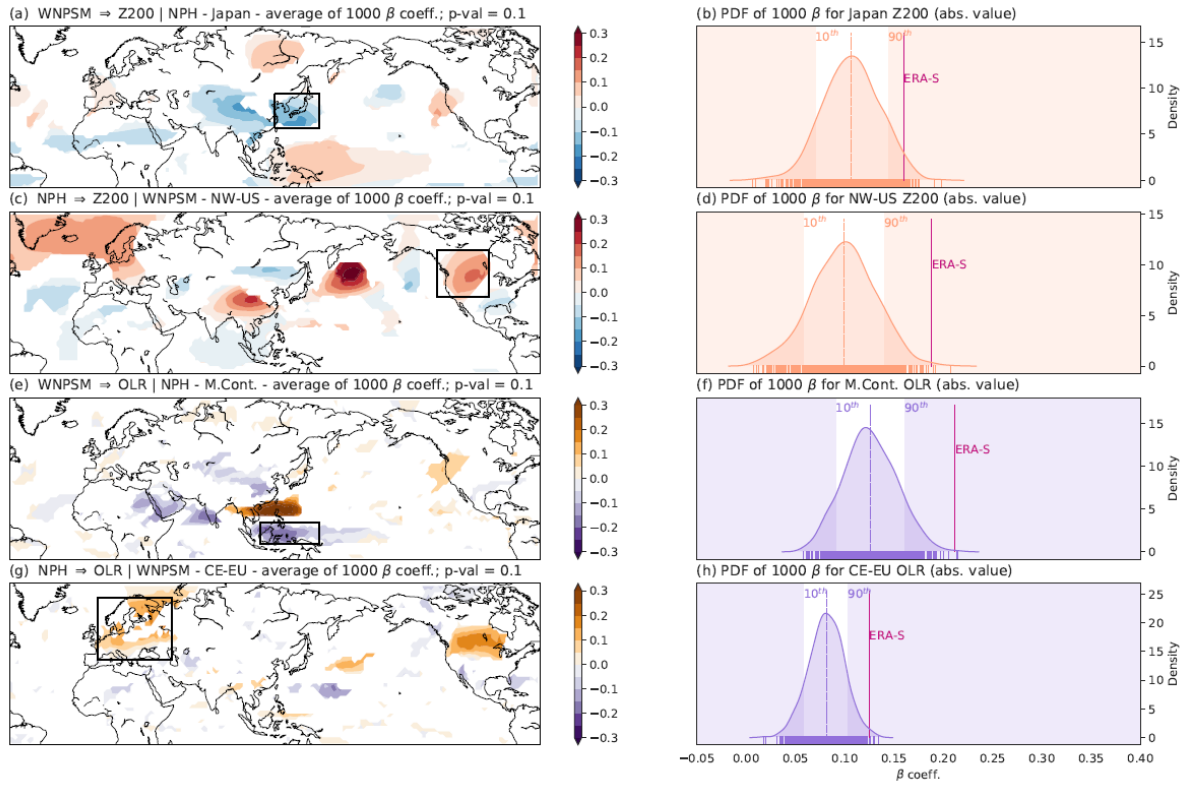


120 **Figure S13.** Same as for Fig. 9 in the main text but obtained with Experiment A.

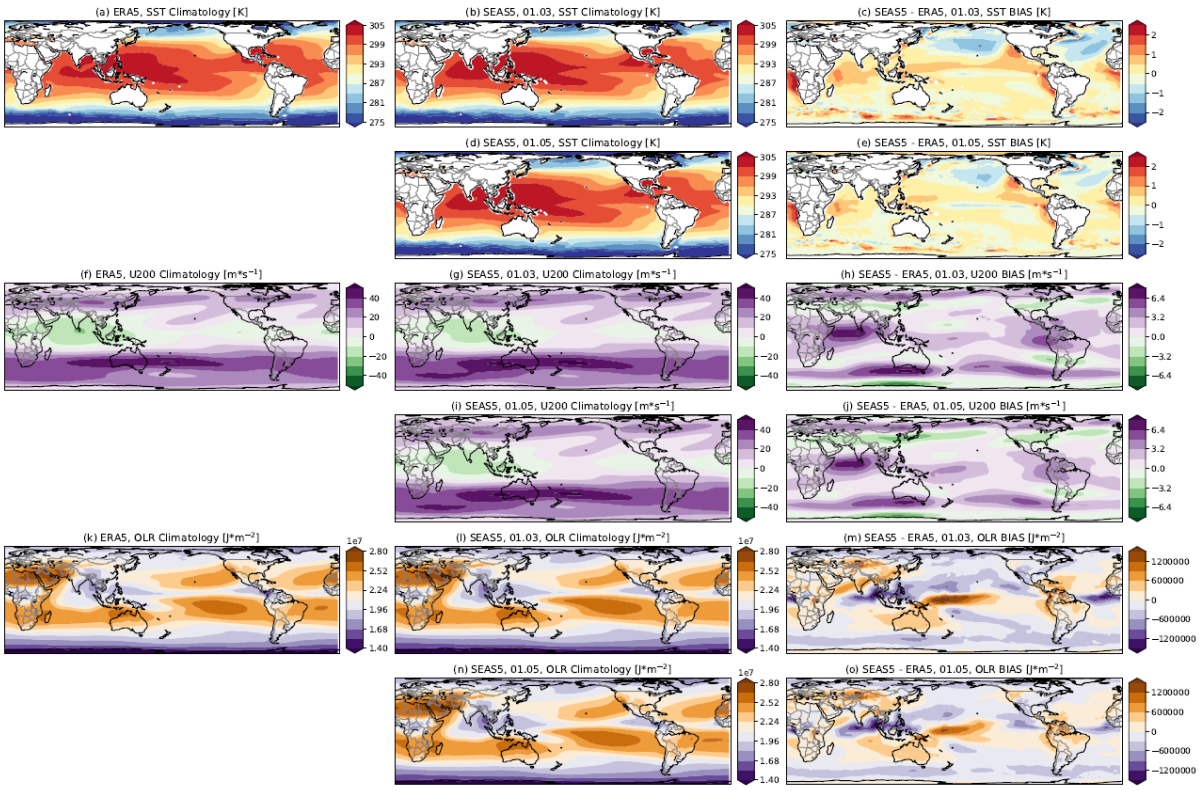


125 **Figure S14.** Bias between ERA5 and SEAS5. Panel (a) shows the JJAS climatology of SST for ERA-S. Panels (b) shows the JJAS climatology of SST for SEAS5 initialized on the 1st of March. Panel (c) shows the BIAS between ERA-S and SEAS5 for SST fields calculated by subtracting ERA-S from the SEAS5 climatology. Panels (d) and (e) same as for panels (b) and (c) but for SEAS5 initialized on the 1st of May. Panels (f)-(j) same as for panels (a)-(e) but for U200 fields. Panels (k)-(o) same as for panels (a)-(e) but for OLR fields.

130

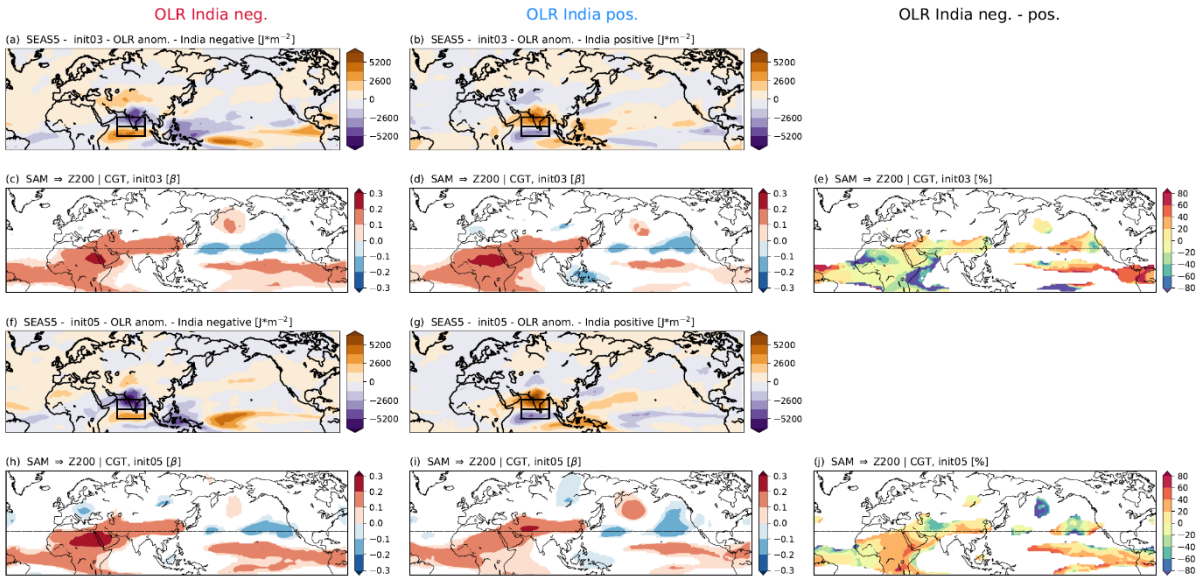


**Figure S15.** Convective activity bias and the Sahel region. Panel (a) shows the composite of JJAS averaged OLR fields for years with negative OLR anomalies over the Indian peninsula for SEAS5 initialized on the 1st of March (94 years in total). Panel (b) same as for panel (a) but for years with positive OLR anomalies over the Indian peninsula (92 years in total). Panel (c) shows the causal map for the link SAM → Z200|CGT obtained with OLR India negative years. Panel (d) same as for panel (c) but for OLR India positive years. Panel (e) shows the difference $\Delta_\beta$ between β values shown in panels (c) and (d). Panels (f) to (j) same as for panels (a) to (e) but for SEAS5 initialized on the 1st of May. For the 1st of May 94 (102) years are detected with negative (positive) OLR anomalies. The black boxes show the two areas used to define the OLR India index (see main text for further description).

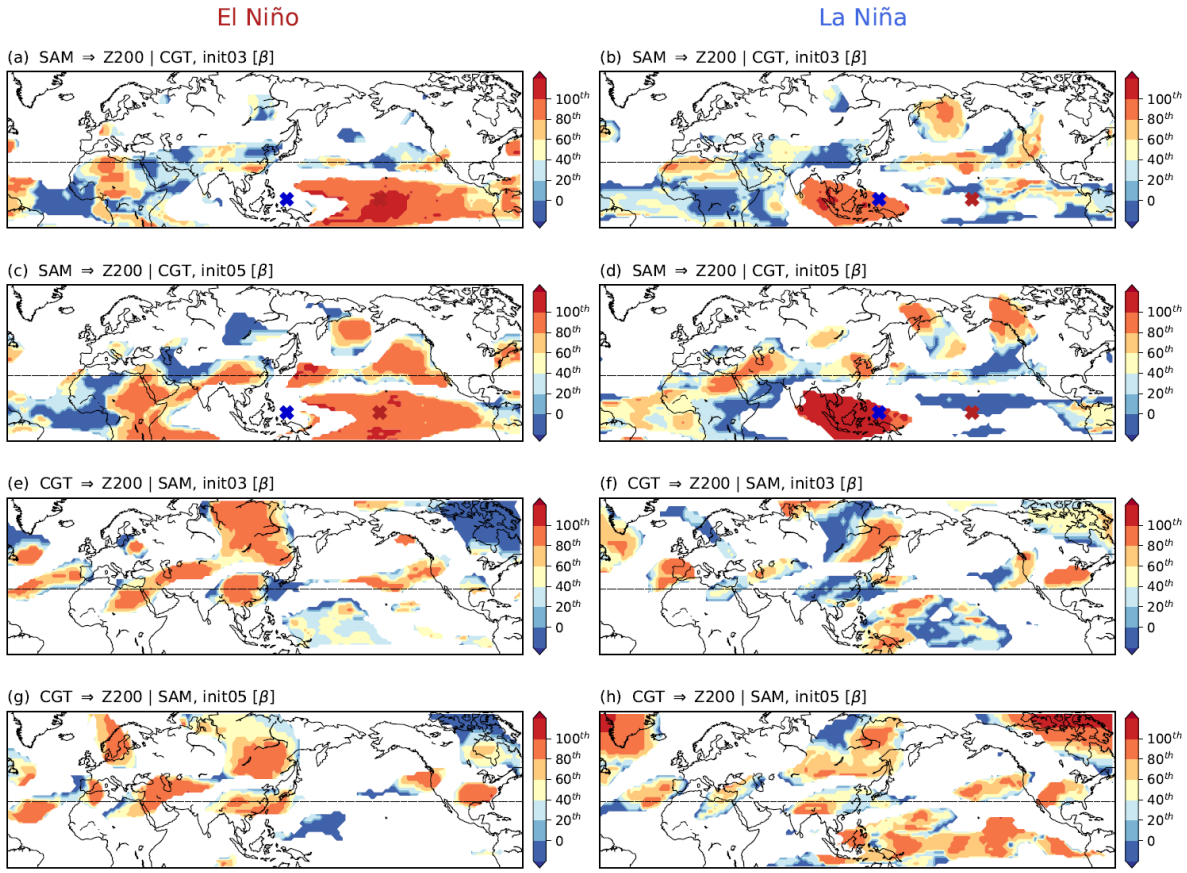


**Figure S16.** ENSO effect on tropical-extratropical links: MCA mode 1. Panels (a) shows the $\beta_{SEAS5}$ calculated during Nino 3.4 positive years compared to $\beta_{SEAS5}$ quantiles obtained by 1000 subsamples of 90 years each for the SAM → Z200|CGT link for SEAS5 data initialized on the 1st of March. Panel (b): same as for panel (a) but for Nino 3.4 negative years. Panel (c) and (d): same as for panels (a) and (b) but for SEAS5 data initialized on the 1st of May. Panels (e) and (f): same as for panels (a) and (b) but for the link CGT → Z200|SAM. Panels (g) and (h): same as for panels (e) and (f) but for SEAS5 data initialized on the 1st of May. Only grid points with corrected *p*-values significant at $\alpha = 0.05$ are shown.

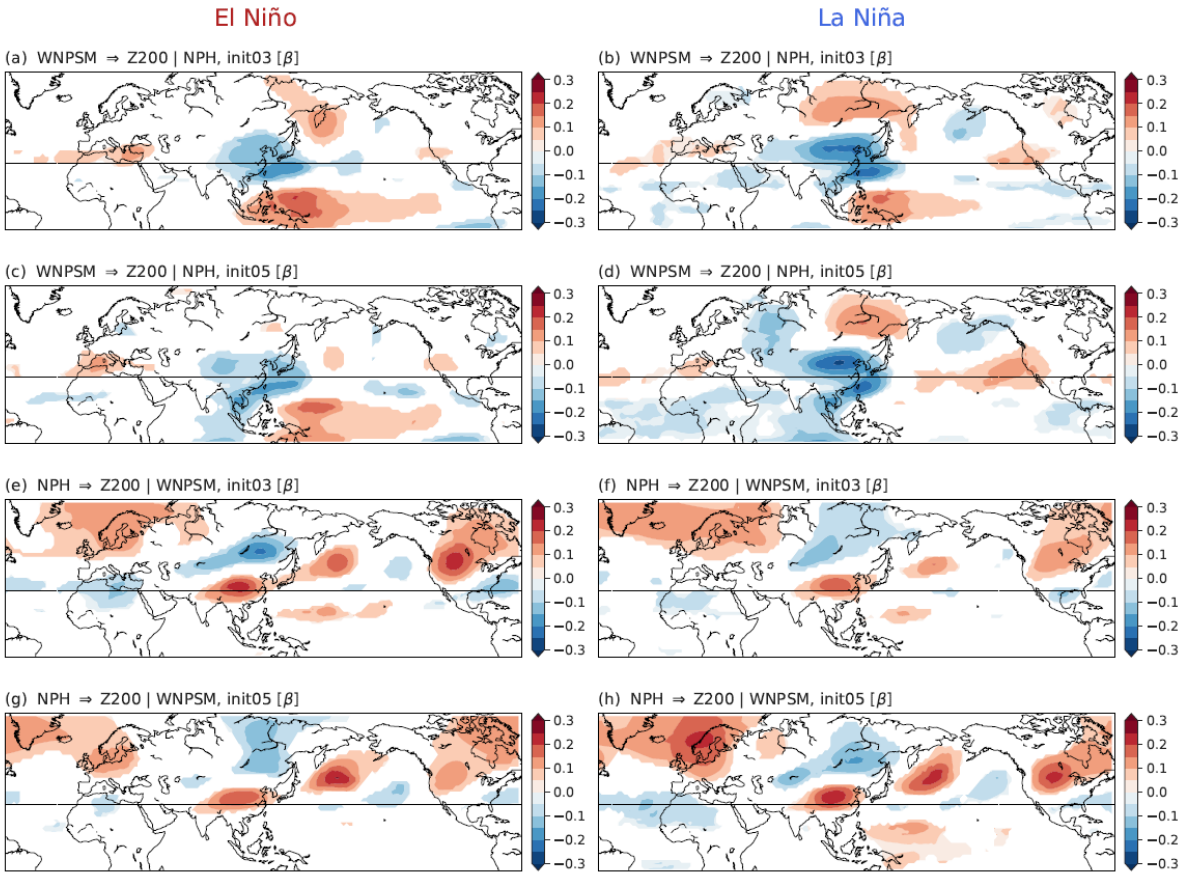


**Figure S17.** ENSO effect on tropical-extratropical links: MCA mode 1. Panels (a) and (b) show the causal maps for SEAS5 data initialized on the 1st of March for the WNPSM → Z200|NHP link respectively during Nino 3.4 positive and negative years. Panel (c) and (d): same as for panels (a) and (b) but for SEAS5 data initialized on the 1st of May. Panels (e) and (f): same as for panels (a) and (b) but for the link NPH → Z200|WNPSM. Panels (g) and (h): same as for panels (e) and (f) but for SEAS5 data initialized on the 1st of May. Only grid points with corrected *p*-values significant at $\alpha = 0.05$ are shown.

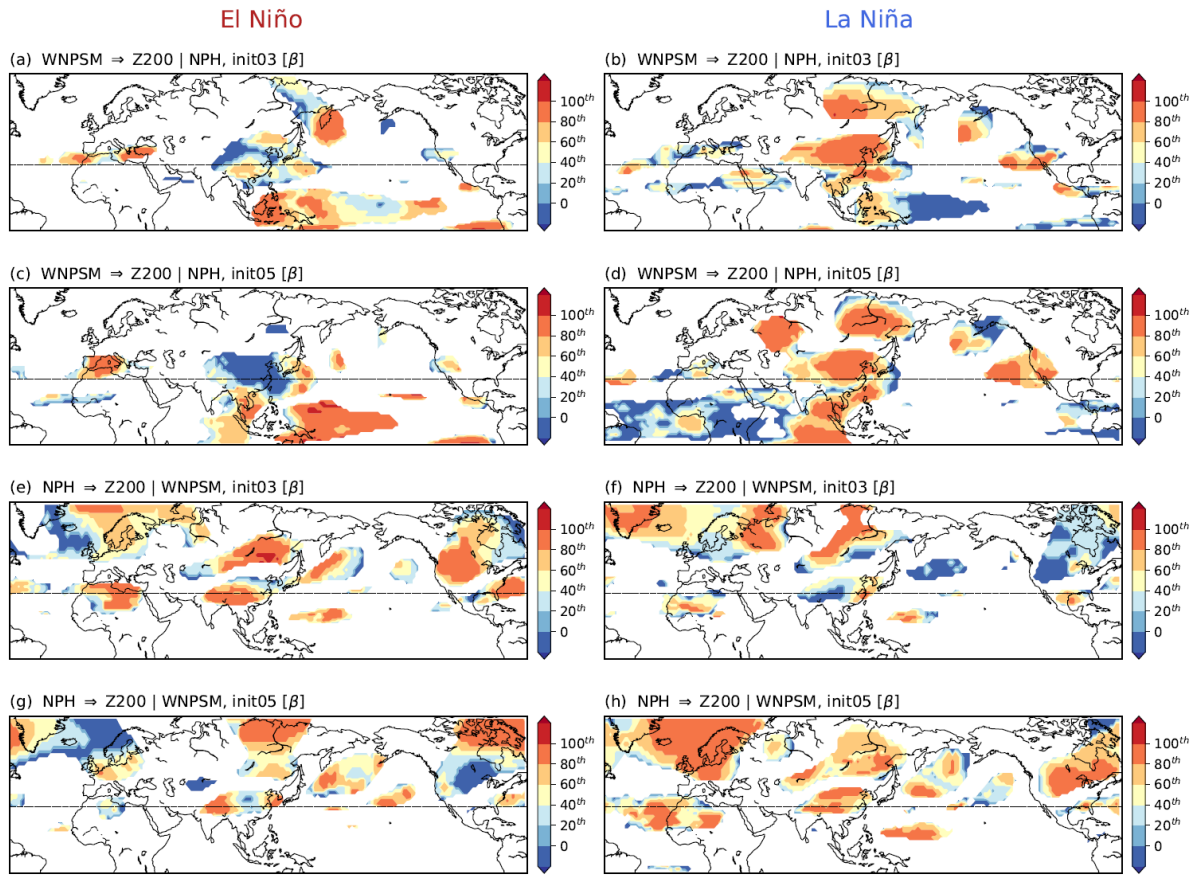


**Figure S18.** ENSO effect on tropical-extratropical links: MCA mode 2. Panels (a) shows the $\beta_{SEAS5}$ calculated during Nino 3.4 positive years compared to $\beta_{SEAS5}$ quantiles obtained by 1000 subsamples of 90 years each for the WNPSM → Z200|NPH link for SEAS5 data initialized on the 1st of March. Panel (b): same as for panel (a) but for Nino 3.4 negative years. Panel (c) and (d): same as for panels (a) and (b) but for SEAS5 data initialized on the 1st of May. Panels (e) and (f): same as for panels (a) and (b) but for the link NPH → Z200|WNPSM. Panels (g) and (h): same as for panels (e) and (f) but for SEAS5 data initialized on the 1st of May. Only grid points with corrected *p*-values significant at α = 0.05 are shown.

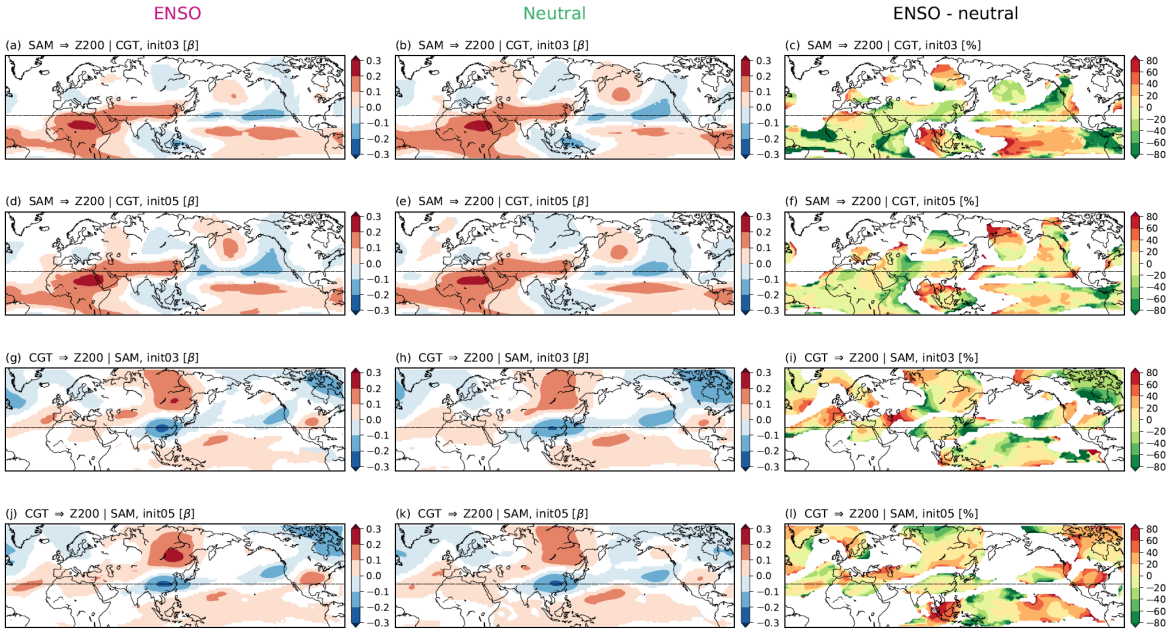


**Figure S19.** Effect of ENSO years and neutral years on tropical-extratropical links: MCA mode 1. Panels (a) and (b) show the causal maps for SEAS5 data initialized on the 1st of March for the SAM → Z200|CGT link respectively during active ENSO years (both El Niño and La Niña together) and neutral years. Panel (c) shows the differences between active ENSO years and neutral years. Panel (d), (e) and (f): same as for panels (a), (b) and (c) but for SEAS5 data initialized on the 1st of May. Panels (g), (h) and (i): same as for panels (a), (b) and (c) but for the link CGT → Z200|SAM. Panels (j), (k) and (l): same as for panels (g), (h) and (i) but for SEAS5 data initialized on the 1st of May. Only grid points with corrected *p*-values significant at $\alpha = 0.05$ are shown.

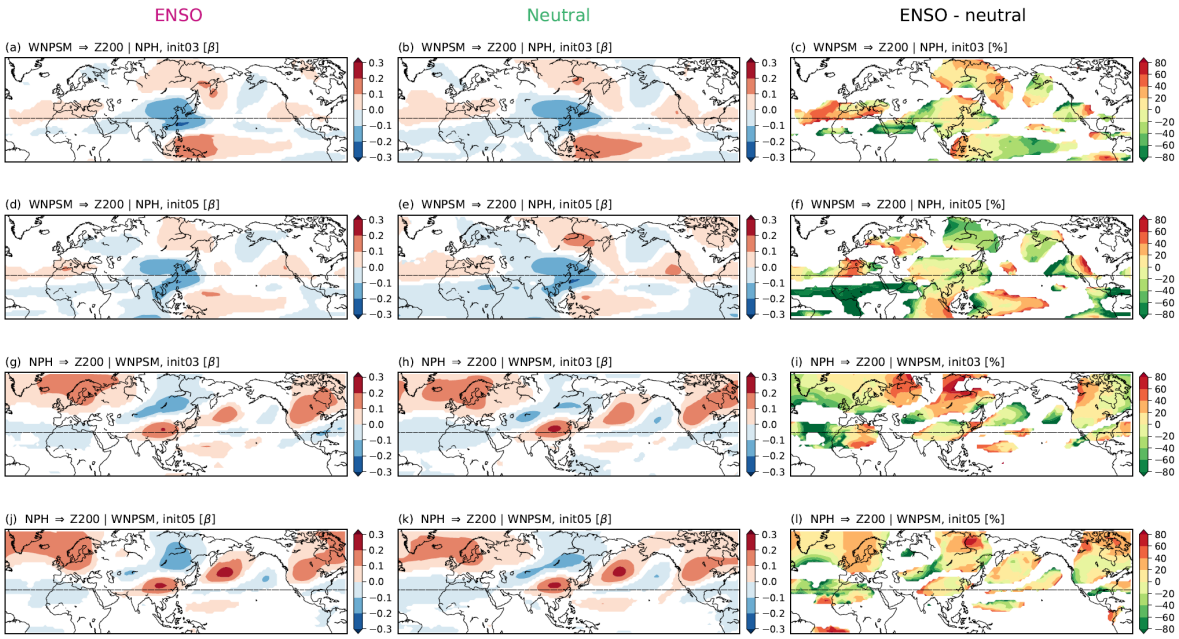


**Figure S20.** Same as for Fig. S19 but for MCA 2.

| ERA-S | Correlation coefficient | p-value |
|---|---|---|
| MCA1 Z200 (CGT) - MCA1 OLR (SAM) | 0.59 | $1.02*10^{-45}$ |
| MCA1 OLR (SAM) - MCA2 OLR (WNPSM) | 0.03 | 0.46 |
| MCA2 Z200 (NPH) - MCA2 OLR (WNPSM) | 0.54 | $4.93*10^{-38}$ |
| MCA1 Z200 (CGT) – MCA2 Z200 (WNPSM) | -0.03 | 0.50 |

180

**Table S1.** Correlation coefficients between different pairs of ERA-S MCA modes.